Journal of the European Ceramic Society 38 (2018) 5058–5066

Contents lists available at ScienceDirect

Journal of the European Ceramic Society

journal homepage: www.elsevier.com/locate/jeurceramsoc

Original Article

Co and Fe co-doping influence on functional properties of $SrTiO_3$ for use as oxygen transport membranes

Yang Liu[a,*], Stefan Baumann[a], Falk Schulze-Küppers[a], David N. Mueller[b], Olivier Guillon[a]

[a] Forschungszentrum Jülich GmbH, Institute of Energy and Climate Research – Materials Synthesis and Processing (IEK-1), Leo-Brandt-Strasse, 52425, Jülich, Germany
[b] Forschungszentrum Jülich GmbH, Peter Grünberg Institute – Electronic Properties (PGI-6), Leo-Brandt-Strasse, 52425, Jülich, Germany

ARTICLE INFO

Keywords:
Oxygen transport membrane
Cobalt doping
Strontium titanate
Conductivity
Permeance

ABSTRACT

Perovskite-structured powders of $SrTi_{1-x}Co_xO_{3}.\delta$ (STC-x) with nominal stoichiometry of x = 0–0.75 as well as $SrTi_{0.75}Co_{0.25-y}Fe_yO_{3}.\delta$ (STCF-y) where y = 0–0.25 were synthesized using the Pechini method. Thermal/chemical expansion behaviour, total electrical conductivities, and oxygen permeation rates were investigated. The substitution of Ti with Co leads to an increase in both electronic and ionic conductivities and, therefore, oxygen permeability. Thermal and chemical expansions also increase slightly. The optimum Co content was found to be 25–35% due to the trade-off between phase stability and permeability. The oxygen permeation rate of STC35 is comparable to that of state-of-the-art $(La,Sr)(Co,Fe)O_{3}.\delta$, whereas the expansion coefficients are lower. Co-doping in STCF-y did not produce any significant differences in oxygen permeability at both high temperature and sample thickness (1.0 mm), i.e. in a solid-state diffusion-limited regime. At lower temperatures (< 800 °C), STC25 exhibits higher permeability than STF25 due to the higher catalytic activity of Co compared to Fe.

1. Introduction

Mixed ionic and electronic conductors (MIEC) have gained much attention due to their potential application in oxygen transport membranes to separate oxygen from air or other oxygen-containing gas mixtures as well as their potential application on membrane reactors for partial oxidation, for example syngas production [1,2]. Moreover, MIEC perovskites are used in electrochemical devices such as solid oxide fuel cell (SOFC) electrodes, particularly cathodes [3,4]. One promising class of membrane materials are the cubic perovskites $ABO_{3-\delta}$, with the A cation at the corner of the cube and the B cation in the centre of the cubic unit cell with oxygen ions in the face-centred positions, leading to the formation of BO_6 octahedra extended three dimensionally. The cubic perovskite structure materials have the advantage of accommodating a number of different cations with different valences in its lattice. In other words, different elements can be doped on the A site or B site to obtain different oxygen stoichiometries, facilitating the formation of oxygen vacancies and electron holes to achieve the desired MIEC behaviour [5]. The $SrFeO_{3-\delta}$- and $SrCoO_{3-\delta}$-based perovskite materials with A site substitutions such as Ba and La were comprehensively investigated. Among them, the $La_{1-x}Sr_xCo_yFe_{1-y}O_{3-\delta}$ (LSCF), $SrCo_{0.8}Fe_{0.2}O_{3-\delta}$, and $Ba_{0.5}Sr_{0.5}Co_{0.8}Fe_{0.2}O_{3-\delta}$ (BSCF) series were reported to have a high oxygen permeation rate [6–10]. However, LSCF and BSCF have low phase stabilities in low oxygen partial pressures [11–13] as well as aggressive gases such as CO, CH_4, and CO_2 [14]. Therefore, B-site doping by Zr, Nb, Ti, and Y, particularly in BSCF, was carried out to improve stability [15–22]. These approaches were successful to a certain extent, but the large amount of Co and Fe in the B site of these materials still leads to limited resistance in reducing environments. In contrast, research was carried out on the perovskite material $SrTiO_3$, which is chemically and structurally very stable but practically impermeable to oxygen. By introducing a limited amount of multivalent Fe into the B site sublattice of TiO_6 octahedra, oxygen vacancies and electron holes are formed, thus leading to an oxygen permeation rate comparable to LSCF [23].

Fig. 1 shows a schematic quasi-ternary phase diagram of $SrCoO_3$, $SrFeO_3$, and $SrTiO_3$. The black dots in the diagram (Fig. 1) represent compositions that were reported in the literature. The quasi-binary system $SrCoO_3$-$SrFeO_3$ (SCF) [24,25] has evidently been comprehensively investigated, including limited B site substitution by Ti [26–30]. Furthermore, the quasi-binary system $SrFeO_3$-$SrTiO_3$ (STF) has also been studied [23,31–34]. The quasi-binary system $SrTiO_3$-$SrCoO_3$ (STC) region with high Ti content has been widely investigated with respect to magnetic properties [35–41]. However, the use of mixed ionic and electronic conductivity for oxygen transport membrane (OTM) materials has not yet been systematically characterized. However, it is known that Co is more effective than Fe in terms of the functionalization of perovskites [42,43]. Therefore, in this paper, compositions of

---

* Corresponding author.
E-mail address: ya.liu@fz-juelich.de (Y. Liu).

https://doi.org/10.1016/j.jeurceramsoc.2018.07.037
Received 14 January 2018; Received in revised form 19 July 2018; Accepted 24 July 2018

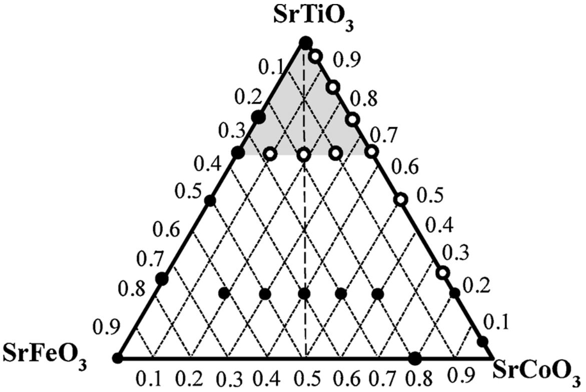

Fig. 1. Quasi-ternary diagram of $SrTiO_3$, $SrFeO_3$, and $SrCoO_3$ showing the compositions investigated in the literature (full circles) and in this study (open circles), respectively [24–29].

$SrTi_{1-x}Co_xO_{3-δ}$ (STC-x) where x = 0, 0.05, 0.15, 0.25, 0.35, 0.5, and 0.75 and compositions of $SrTi_{0.75}Co_{0.25-y}Fe_yO_{3-δ}$ (STCF-y) where y = 0, 0.06, 0.125, and 0.19 were investigated in terms of their functional and manufacturing properties (open dots in Fig. 1). The effect of Co doping and Fe/Co co-doping in STO on oxygen permeation, electrical conductivity, and thermal/chemical expansion behaviour is discussed.

2. Experimental

2.1. Powder preparation

$SrTi_{1-x}Co_xO_{3-δ}$ (x = 0.05, 0.15, 0.25, 0.35, 0.5, 0.75) and $SrTi_{0.75}Co_{0.25-y}Fe_yO_{3-δ}$ (y = 0.06, 0.125, 0.19) powders were prepared using the Pechini synthesis method. Firstly, Ti^{4+} aqueous solution stabilized with nitric acid was obtained by removing the organic part of Titanium(IV) isopropoxide ($Ti[OCH(CH_3)_2]_4$) (Sigma Aldrich) in deionized water. $Sr(NO_3)_2$, $Co(NO_3)_2.6H_2O$, and $Fe(NO_3)_3.9H_2O$ (Merck KGaA) were dissolved in deionized water and the stabilized Ti^{4+} aqueous solution was added. Citric acid (Merck KGaA) was also added for complexation and ethylene glycol (Merck KGaA) was added for polymerization. After polymerization and the evaporation of water from the solution, the formed gel was heated at 600 °C to remove the organic compounds. The powders were then calcined at 950 °C for 5 h to obtain the pure cubic perovskite phase.

In order to achieve a powder with monomodal and narrow particle size distribution, all calcined powders were milled in ethanol with 3 mm ZrO_2 balls for 24 h. The weight ratio of the powder, ethanol, and balls was 1:2:3. The dry powder agglomerates were subsequently crushed in an Agate mortar and sieved through a 200 μm mesh.

The as-prepared powder was then pressed to be sintered at different temperatures ranging from 1280 °C to 1400 °C, dwelling for 10 h to achieve relative densities higher than 98%. Sintering parameters of the samples are shown in Table 1.

2.2. Characterization

The chemical compositions of the synthesized powders calcined at 950 °C were measured by inductively coupled plasma optical emission spectrometry (ICP-OES). Specific surface areas of the calcined and ball-milled powders were determined in an AreaMeter (Ströhlein, Germany) by nitrogen adsorption and particle size distribution by laser granulometry using a Horiba LA-950V2 device. The phase composition of the calcined powder was characterized by X-ray powder diffraction (XRD) (D4 ENDEAVOR diffractometer by Bruker XS with $CuK_α$ radiation (λ = 1.54 Å)). In addition, the morphology of the as-prepared powder was characterized by means of scanning electron microscopy (Zeiss Ultra55).

The relative density of the sintered samples was measured using the method of Archimedes. In order to investigate the thermal/chemical expansion behaviour of sintered samples, 25-mm-long sintered-bar-shaped samples were tested in a Netzsch 402C dilatometer with a heating and cooling rate of 3 °C/min up to 1000 °C in synthetic air using F_{air} = 100 ml/min. Electrical conductivities of the STC-x and STCF-y samples were determined using the 4-point-probe conductivity method in the temperature range of 650 °C to 875 °C. Oxygen permeation measurements of 1.0-mm-thick disc-shaped membranes with a 14.7 mm diameter were conducted in air/Ar oxygen partial pressure gradients at a constant flow rate of 250 ml/min of ambient air as a feed gas and 50 ml/min of Ar as a sweep gas, as was reported elsewhere [23]. The temperature was varied between 1000 °C and 650 °C. Samples were ground with P1200 emery paper prior to oxygen permeation measurements to remove possible contaminations from sintering and to provide a defined thickness and comparable surface roughness. Gold rings with an inner diameter of 13 mm were used to seal the samples to the gasket of the quartz glass reactor at approx. 1000 °C, resulting in an exposed membrane surface area of approx. 1.33 cm^2.

3. Results and discussion

3.1. Powder characterization

The particle size distribution, specific surface area, and lattice parameters of the calcined (950 °C) powders as well as the sintering temperature required to obtain highly dense samples (> 98% of theoretical density) are shown in Table 1. The d_{50} values are around 2 μm and the specific surface areas are around 1–5 m^2/g. ICP-OES results (not shown here) confirmed the desired composition of Sr, Ti, Co, and Fe.

Fig. 2 shows SEM images of the calcined STC25 and STCF12.5 powders, which are representative of all powders. The images reveal that the powders consist of dense agglomerates of nanosized primary particles, which is typical for the Pechini method.

XRD patterns of the powders calcined at 950 °C where x ≤ 0.50 indicate a perovskite structure, as shown in Fig. 3, whereas in a high Co concentration where x < 0.5, the STC-x material exhibited a secondary phase in addition to the perovskite structure. Furthermore, samples with a high Co content (x ≥ 0.5) showed instability in ambient air at

Table 1
Particle size distribution, specific surface area of processed powder, and sintering temperature of the samples.

Name	Composition	d_{10} μm	d_{50} μm	d_{90} μm	Spec. surface area m^2/g	Sintering temperature (°C)
STC05	$SrTi_{0.95}Co_{0.05}O_{3-δ}$	0.39	2.53	7.13	1.4	1400
STC15	$SrTi_{0.85}Co_{0.15}O_{3-δ}$	0.84	2.43	6.61	2.4	1400
STC25	$SrTi_{0.75}Co_{0.25}O_{3-δ}$	0.89	2.68	6.38	4.4	1280
STC35	$SrTi_{0.65}Co_{0.35}O_{3-δ}$	0.79	2.21	5.93	4.5	1250
STC50	$SrTi_{0.50}Co_{0.50}O_{3-δ}$	0.78	2.09	4.90	4.8	1200
STC75	$SrTi_{0.25}Co_{0.75}O_{3-δ}$	0.69	1.62	4.02	5.9	1150
STCF19	$SrTi_{0.75}Co_{0.06}Fe_{0.19}O_{3-δ}$	0.68	1.99	4.91	5.7	1300
STCF12.5	$SrTi_{0.75}Co_{0.125}Fe_{0.125}O_{3-δ}$	0.64	2.16	5.789	3.4	1300
STCF6	$SrTi_{0.75}Co_{0.19}Fe_{0.06}O_{3-δ}$	0.63	2.35	5.65	4.4	1300